The Birth of Nickel Phosphide Catalysts: Monitoring Phosphorus Insertion into Nickel

Sophie Carenco, Zhi Liu, Miquel Salmeron

▶ **To cite this version:**

Sophie Carenco, Zhi Liu, Miquel Salmeron. The Birth of Nickel Phosphide Catalysts: Monitoring Phosphorus Insertion into Nickel. ChemCatChem, 2017, 10.1002/cctc.201601526 . hal-01520242

HAL Id: hal-01520242

https://hal.sorbonne-universite.fr/hal-01520242v1

Submitted on 10 May 2017

HAL is a multi-disciplinary open access archive for the deposit and dissemination of scientific research documents, whether they are published or not. The documents may come from teaching and research institutions in France or abroad, or from public or private research centers.

L'archive ouverte pluridisciplinaire **HAL**, est destinée au dépôt et à la diffusion de documents scientifiques de niveau recherche, publiés ou non, émanant des établissements d'enseignement et de recherche français ou étrangers, des laboratoires publics ou privés.

The Birth of Nickel Phosphides Catalysts: Monitoring Phosphorus Insertion into Nickel

Sophie Carenco,[1,] Zhi Liu,[2,3] Miquel Salmeron[4,5]*

[1] Sorbonne Universités, UPMC Univ Paris 06, CNRS, Collège de France, Laboratoire de Chimie de la Matière Condensée de Paris, 4 Place Jussieu, 75005 Paris, France

[2] Division of Condensed Matter Physics and Photon Science, School of Physical Science and Technology, ShanghaiTech University, Shanghai 200031, China.

[3] State key Laboratory of Functional Materials for Informatics, Shanghai Institute of Microsystem and Information Technology, Chinese Academy of Sciences, Shanghai 200050, China.

[4] Chemical Sciences Division, Lawrence Berkeley National Lab, Berkeley, California, United States.

[5] Material Sciences Division, Lawrence Berkeley National Lab, Berkeley, California, United States.

E-mail: sophie.carenco@upmc.fr

Abstract: Tri-n-octylphosphine (TOP) is widely used as a phosphorating agent to yield metal phosphide nanocatalysts, which are receiving intense attention because of their high performance in both electrochemical and hydrotreatment catalytic processes, such as the hydrogen evolution reaction and the hydrodesulfurization reaction. Using *in situ* ambient-pressure X-ray photoelectron spectroscopy, the formation of nickel phosphide on the surface of a nickel foil was investigated, at temperatures like those employed to form nickel phosphide nanoparticles in the colloidal route. We uncovered that the onset of phosphorus insertion into nickel is as low as 150 °C, much lower than reported in the literature

(> 210 °C). Moreover, formation of sp2 carbon was observed on the surface as the consequence of TOP alkyl chain decomposition. These findings provide new insight on the surface chemistry of metal phosphide nanoparticles, increasingly employed in several fields of catalysis. Our results demonstrate that even below 150 °C, significant phosphorus and carbon incorporation can occur during metal nanoparticles syntheses that employ TOP as stabilizing agent.

Key-words: nickel phosphide, surface state, *in situ* ambient-pressure XPS, tri-n-octylphosphine.

1. Introduction

Metal phosphide (M_xP_y) nanoparticles are gaining a lot of attention, because of their interesting performance in many applications such as energy storage,[1,2] catalysis,[3,4],[5] optics,[6,7] magnetism,[8,9] etc.[10] More recently, Ni_2P and CoP, amongst other metal phosphide nanoparticles, were shown to be excellent materials for the hydrogen evolution reaction (HER), resulting in a strong development in the last four years.[11–18]

The importance of composition, surface chemistry and possible impurities in electrochemical applications makes it mandatory to develop in-depth understanding of the mechanism of formation of the active nanoparticles. For example, nanoparticles of Ni_2P, $Ni_{12}P_5$ and Ni_5P_4 showed contrasted performances in HER.[17] On the broader picture, gaining a better understanding of the surface chemistry of metal phosphides produced by colloidal routes is essential to their development in other branches of catalysis, eg. hydrotreatment[3] or selective hydrogenation reactions.[5,19,20]

The typical synthesis for metal phosphide nanoparticles employs tri-n-octylphosphine (TOP) both as a surface stabilizing agent and as a source of phosphorus in a reaction that is performed above 250 °C in most cases, under atmospheric pressure.[10,21–23],[24] This route was used for a range of metals, and in particular for nickel, producing Ni_2P or $Ni_{12}P_5$ nanoparticles depending on the reaction conditions.[25,26] *Ex situ* x-ray absorption (XANES and EXAFS) was performed on intermediary products in the synthesis of nickel and cobalt phosphide nanoparticles, in order to identify the decomposition temperature of TOP. For cobalt phosphide, Ha et al. showed that at 300 °C TOP decomposes within minutes.[27] For nickel phosphide, Seo et al. found the decomposition temperature to be above 250 °C[28] in a synthesis

method where oleylamine was not used as the reducing agent. In the presence of this reducing agent, nickel nanoparticles start forming at 213 °C[29],[30] and can catalyze the decomposition of the phosphine. Moreau et al. showed that 230 °C is enough for decomposing TOP and crystallizing the phosphide,[31] even though phosphorus doping already happens at a temperature as low as 210 °C.[32] From a structural stand-point, this mechanistic study also showed that the phosphorus first inserts in the nickel in substitutional sites, and not in interstitial sites. However, because the analysis was done *ex situ* and on nanoparticles that were washed and isolated, it was still difficult (1) to determine the onset temperature of P–C bond breaking in TOP, and (2) to identify the carbon surface species that could form as a result of this bond breaking. Yet, surface state is crucial to the catalytic activity of nickel phosphide catalysts, both in electrochemical (hydrogen evolution reaction)[14] and chemical (hydrodesulfurization reaction) processes.[33]

More generally, monitoring TOP decomposition is also relevant because this molecule is used as a surface ligand for many metal(0) nanoparticles[34] that are employed in catalytic reactions such as Fischer-Tropsch and CO_2 reduction. In several cases phosphorus contamination was detected, which was shown to strongly impact the catalytic activity and selectivity.[35,36]

In this study, we employed ambient-pressure X-ray photoelectron spectroscopy (APXPS)[37] as an *in situ* tool to monitor the decomposition of TOP at the same temperature range as that in colloidal synthesis. A nickel foil was used as a model for nickel nanoparticles and the decomposition of TOP was achieved in reducing conditions under 100 mTorr of H_2. We found that the onset of phosphide formation was as low as 150 °C. Additionally, significant amounts of carbon in sp2 form were found to accumulate on the surface as a result of TOP decomposition.

2. Results and discussion

2.1 Adsorption of TOP on nickel

From nanoparticle to foil. For a typical synthesis of nickel phosphide nanoparticles, a source of nickel(II) such as nickel(II) acetylacetonate is reacted with a reducing agent (oleylamine) in the presence of TOP as a surface ligand and source of phosphorus (Scheme 1A).[25]

In order to study the decomposition of TOP on nickel, a foil of the metal was used for two reasons. (1) The temperature of decomposition of TOP is expected at around 210-230 °C[32] and at this temperature nickel(II) quickly reduces to nickel(0) nanoparticles,[30] hence a nickel foil surface should be a good model. (2) In contrast to a single-crystal surface, the nickel foil exhibits a variety of surface structures that can model the nanoparticle edges, corners and defects.

At beamline 9.3.2 of the Advanced Light Source (ALS, Berkeley),[38] a nickel foil was cleaned using cycles of sputtering and annealing. Under N_2 atmosphere, the foil was taken out of the preparation chamber and TOP was deposited using a diluted solution in dry and degassed toluene, a volatile solvent (Scheme 1B). At the working pressure, TOP does not evaporate and stays adsorbed on the surface, thus mimicking atmospheric pressure colloidal experiments.

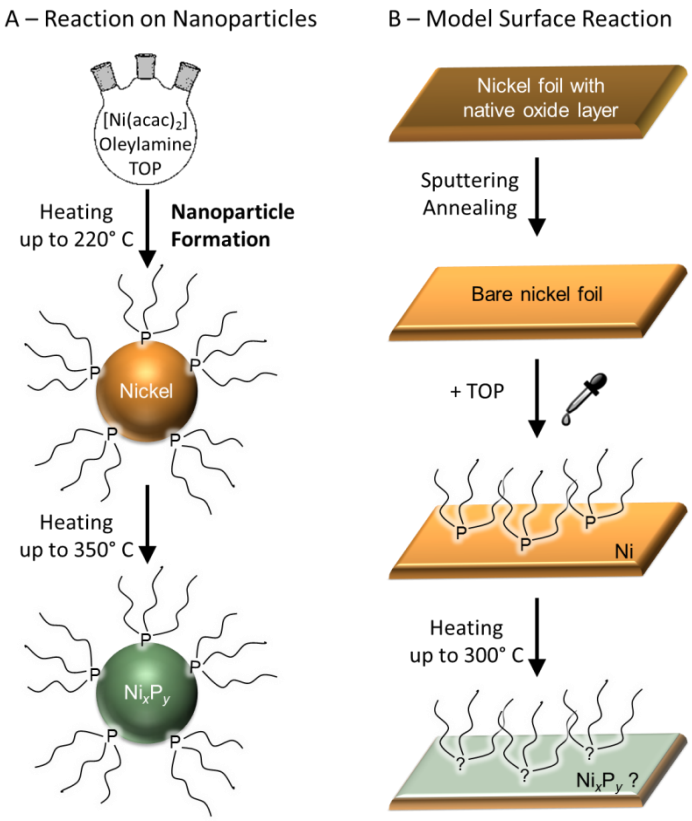

Scheme 1: (A) Typical literature procedure for preparing nickel phosphide nano-catalysts from tri-n-octylphosphine (TOP). (B) Surface processing steps to study insertion of phosphorus from TOP to nickel.

Surface state of TOP-covered nickel foil

XPS was performed on the nickel foil prior (Figure 1, lower spectra, and Figure S1) and after (Figure 1, upper spectra) TOP adsorption. For XPS peaks with spin-orbit doublets, only the position of the component at lower binding energy (B.E.) is indicated in the discussion (see ESI for fitting parameters).

With a single peak at a B.E. of 110.6 eV and its satellite at 116.0 eV, Ni 3s region shows that the foil is in a metallic state prior to deposition of TOP.[39] This is confirmed in the Ni 3p region by the presence of a peak at 66.0 eV (in green) for Ni $3p_{3/2}$, and a broad satellite at 71 eV (in dark green).[39]

As a result of the deposition procedure, phosphorus can be observed in the P 2p region with two doublet peaks, at 132.1 (ochre) and 133.0 eV (yellow). The first is consistent with phosphine coordinated to metal,[40] the other could be due to a different coordination mode of the phosphine to unsaturated sites on the surface of the nickel foil. Partial oxidation of the surface was observed by the appearance of nickel oxide peaks (in dark green) at 112.5 eV (satellite at 119 eV) in Ni 3s region and a peak at 68.9 eV (satellite at 72.5 eV) in the Ni 3p region, in agreement with ref [41]. Consistently, an oxide peak appeared in the O1s region at 529.9 eV (dark green). In this region, two other components appeared at 531.7 eV (ochre) and at 533.0 eV (yellow) probably due to hydroxyls and water, which is present in trace amounts in the toluene solvent and in the glovebag used for deposition of TOP. Alkyl chains of TOP are observed in the C 1s region by a peak at 285.6 eV (in brown). This region also shows additional components after adsorption: at 283.8 eV (in ochre), 284.7 eV in green, 286.7, 288.1 and 289.4 eV in yellow. Detailed attribution for C 1s peaks will be discussed in the next section.

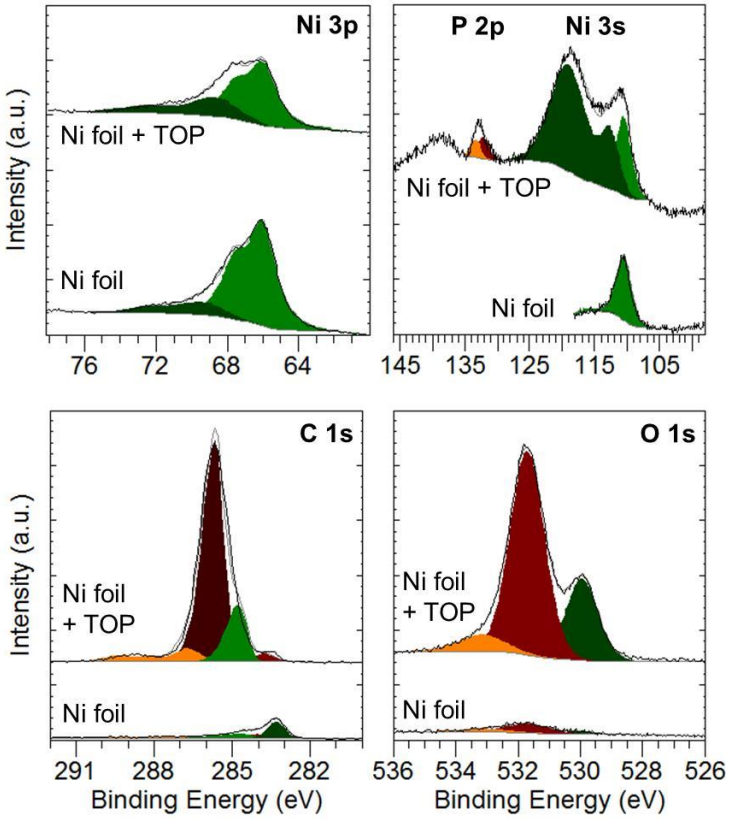

Figure 1: XPS of nickel foil under UHV, before and after addition of TOP. Color code is the following: Ni 3p and Ni 3s: Ni(0) in green and nickel oxide in dark green; P 2p: TOP on nickel in ochre and TOP on unsaturated sites in yellow; C 1s: foil native carbide in ochre, TOP alkyl chains in brown, all C-O species in yellow, sp2 carbon on nickel in green; O 1s: oxide in dark green, hydroxyl and carbonates in ochre, adsorbed water in yellow (see Supplementary Information).

The presence of phosphine on the surface is attested by the XPS peaks in the P 2p region. A free alkyl-phosphine would have given a peak in the range 130 – 131 eV,[42,43] which was not observed. As the phosphine was introduced in fairly low amounts *vs.* the nickel (less than a monolayer), the spectra also highlights the high sensitivity of the nickel foil and its tendency to adsorb any other possible molecule to saturate its surface. The presence of these additional species is not an obstacle for modeling the nickel nanoparticles: in a reaction flask, oxygen-containing molecules (ketones) and even water molecules generated *in situ*[30] are present and also adsorb on the nanoparticles surface.

2.2 The onset of TOP decomposition

Due to the high reactivity of the Ni foil, oxidation arising from traces of H_2O present in the UHV chamber is expected. Moreover, in the reaction flask the thermal decomposition of oleylamine provides a reductive environment for the nickel nanoparticles.[30] For these two reasons, the decomposition of TOP was studied under slightly reducing conditions in a 100 mTorr of H_2 background. The foil modified with TOP was heated to 100 °C, then to 150 °C, while collecting XPS of P 2p and Ni 3s regions (Figure 2). The surface is similar at r.t. and 100 °C, except for a slightly higher amount of reduced nickel at 100 °C (lighter green component of Figure 2b). At 150 °C, significant changes are observed (Figure 2c). First, the nickel reduction is more pronounced. Second, a new phosphorus peak appears at 129.3 eV (in brown), consistent with the formation of a nickel-rich phosphide alloy at the surface (129.3-129.4 eV).[44] This peak position is close to that of crystalline phases of Ni_2P and Ni_5P_4 (129.5 eV).[45]

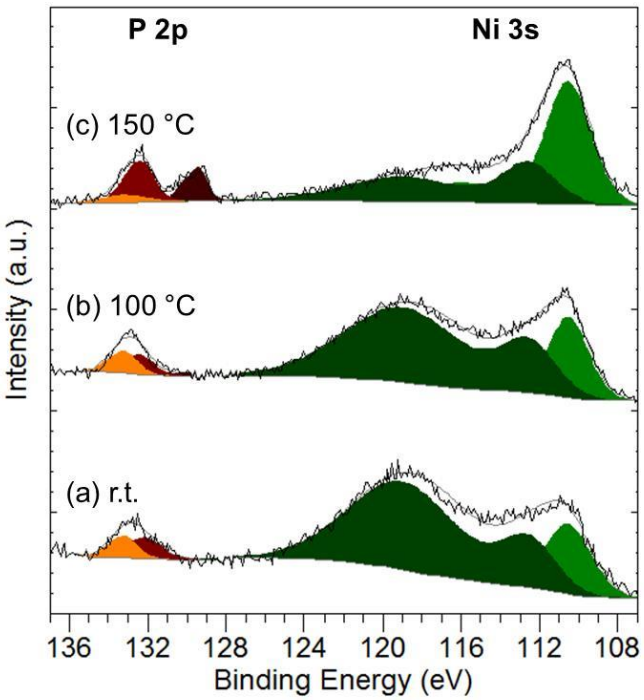

Figure 2: XPS of TOP-covered nickel foil under 100 mTorr of H_2, at r.t. (a) then upon heating at 100 °C (b) and 150 °C (c). Nickel phosphide is observed at 129.2 eV (dark brown) on spectrum (c). Color code: Ni 3s: Ni(0) in green and nickel oxide in dark green; P 2p: TOP on nickel in ochre, TOP on unsaturated sites in yellow, nickel phosphide in brown.

This experiment demonstrates that, in the presence of metallic nickel, TOP can already decompose and provide phosphorus atoms to the metal at 150 °C, a much lower temperature than anticipated from previous works (210 – 250 °C).[28],[31] However, 210 °C is also the temperature typically required to start forming nickel(0) species in the reaction medium. This strongly suggests that the nickel(0) surface acts as catalyst for breaking the P–C bonds of TOP. Such reactivity is consistent with observations made on nickel(0) organometallic complexes containing phosphine ligands:[46] P–C bond cleavage were observed at temperatures as low as 100 °C.[47]

In summary, this first experiment allowed identifying an onset temperature for TOP decomposition of 150 °C. We can further propose that once nickel(0) is present in the reaction flask, the phosphidation reaction could be achieved at a temperature lower than 210 °C. To confirm this, we monitored the time evolution of the foil phosphidation at 150 °C.

2.3 Further phosphidation and identification of carbon species

Figure 3a-c shows the evolution of the surface at 150 °C. Spectra were collected with intervals of 25 minutes. Below the spectra, are plotted the relative ratio of the species, based on C 1s region (left) and P 2p region (right), calculated from the area of the fitted peaks. From spectrum (a) to spectrum (c), the amount of phosphide slightly increases from 33 to 42 %, indicating a slow decomposition of TOP at 150 °C. When the temperature increased to 200 °C (spectra d-f), 250 °C (spectra g-i) and then 300 °C (spectra j-k), the formation of phosphide was more pronounced. This species represent 75 % of the phosphorus on spectrum k. On the C 1s chart, the species at 284.7 eV was observed to increase at a similar rate (reaching 64 % on spectrum k), while the species at 285.6 eV (alkyl chains from TOP) decreases. Contributions at 283.8 eV, attributed to carbide, and above 286 eV, attributed to carbonate-type species, are not significantly modified in the process. Hence, we propose that the peak at 284.7 eV corresponds to species formed by the decomposition of TOP alkyl chains. Because nickel thin films and nanoparticles are typically used as catalysts for carbon nanotubes formation in CVD processes,[48,49] our interpretation is that the decomposition of sp3 carbon from TOP leads to the formation of sp2 carbon on the surface. Consistently, the peak position (284.7 eV) has a B.E. close to sp2 carbon in nickel

cyclopentadienyl complex (reported at 284.9 eV).[50] Lastly, at 300 °C, almost all alkyl chains of TOP are decomposed, as shown by the disappearance of the peak at 285.6 eV (brown), but phosphine-type coordination can still be observed from the peak at 132.1 eV, indicative of the presence of P(III) species. This is unexpected and suggests that the carbon chains of the phosphine decompose faster than the P–C bond. As noted by Schaefer et al.,[51] in similar reaction conditions, carbon doping occurs in nickel nanoparticles. Moreover, the formation of short alkyl and alkene chains[46] likely leads to the desorption of part of the carbonated species. Consistently, phosphidation and sp2 carbon concomitantly increase from 33 to 75 % and from 34 to 64 %, respectively, with a rate that is slightly lower for sp2 carbon. This shows that TOP should not only be considered as a source of phosphorus during nanoparticle syntheses, but also as a carbon source.

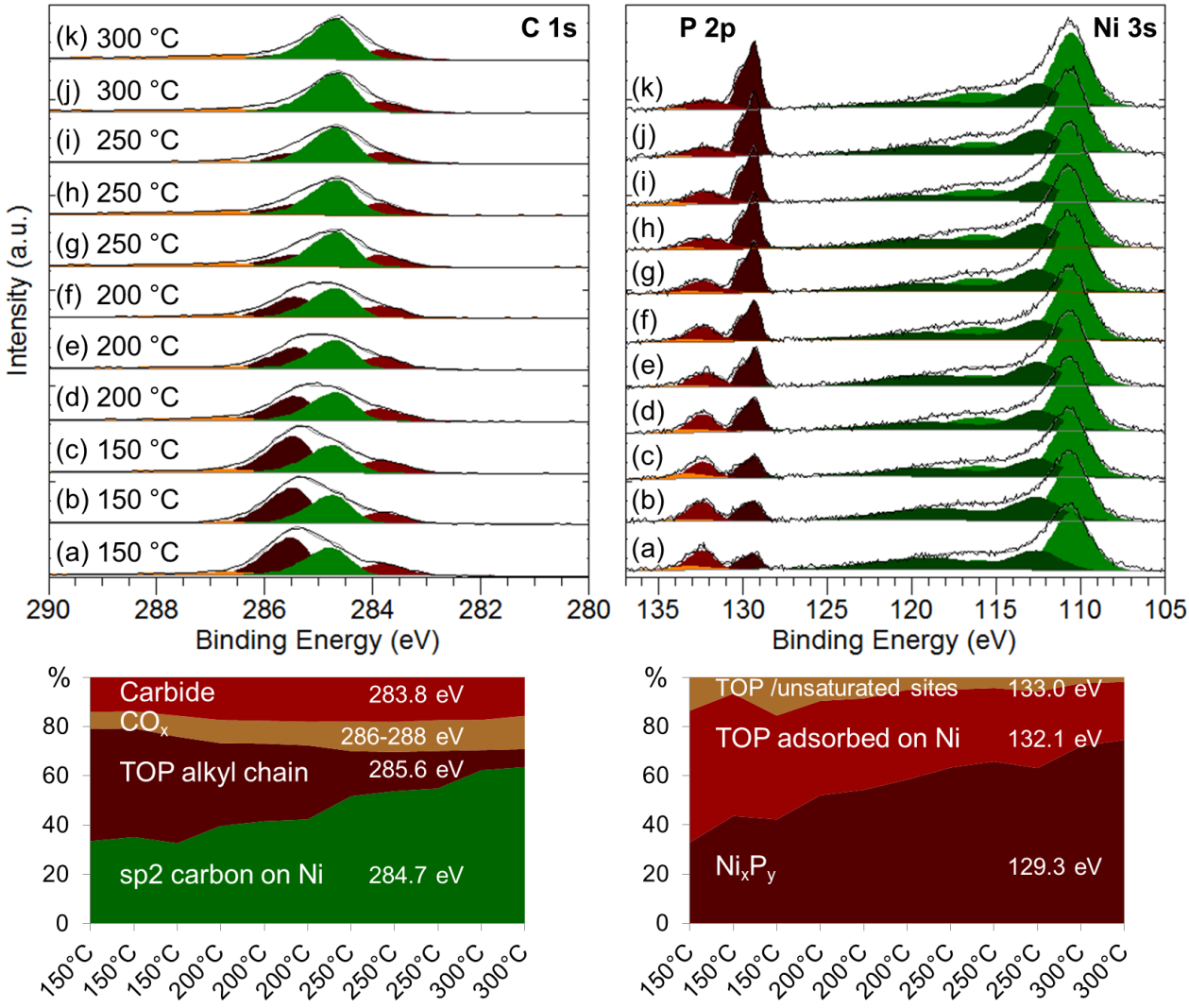

Figure 3: (Top) XPS of TOP-covered nickel foil under 100 mTorr of H_2, from r.t. up to 300 °C (a-k). (Bottom left) Relative area of the carbon species. (Bottom right) Relative area of the phosphorated species. Color code is the following: Ni 3s: Ni(0) in green and nickel oxide in dark green; P 2p: TOP on nickel in ochre, TOP on unsaturated sites in yellow, nickel phosphide in brown; C 1s: carbide in ochre, TOP alkyl chains in brown, all C-O species in yellow, sp2 carbon on nickel in green.

2.4 Comparison with a colloidal experiment on nickel(0) fcc nanoparticles

In order to confront our findings to the situation of colloids in solution, we prepared under inert atmosphere Ni(0) fcc nanoparticles from the reduction of [Ni^{II}(acetylacetonate)$_2$] by oleylamine at 220 °C but in the absence of TOP, a reaction that is quantitative and well-controlled.[52,53] Then, TOP (5 equivalents *vs.* nickel) was added to the solution at room temperature. This solution was heated at

150 °C for 4h, during which TOP was able to react with the surface of the nickel(0) nanoparticles (Figure 4A). The nanoparticles were collected by centrifugation and washed three times. They were analyzed by transmission electron microscopy (Figure 4B), X-ray diffraction on powder (Figure 4C) and XPS (Figure 4D).

The nanoparticles diameter was in the range 50-80 nm, as expected from this synthetic route (Figure 4B and Figure S2).[52] However, x-ray diffraction (Figure 4C) showed the presence of nickel carbide in addition to the expected nickel fcc phase. This shows that ligand decomposition (here, TOP and/or oleylamine) leads to C-C bond breaking at 150 °C. Carbide species along with carbon sp2 species were also observed by *ex situ* C 1s XPS by the two peaks at 283.8 and 284.8 eV, respectively (Figure 4D). P 2p region also revealed the presence of a species at 129.9 eV, which we attribute to a phosphide layer. Altogether, this control experiment on nickel nanoparticles confirmed the reactivity of TOP at 150 °C toward nickel(0) species. Such reactivity was not identified before, because in typical synthesis the nickel precursors (eg. [Ni^{II}(acetylacetonate)$_2$]) are Ni(II) species, which require higher temperatures such as 213 °C to be reduced to nickel(0).[53] Here, the nickel(0) nanoparticles were formed in a first step at 220 °C in the absence of TOP, and then the solution was cooled down before adding TOP: the reactivity observed with TOP necessarily occurred during the 4h-reaction at 150 °C.

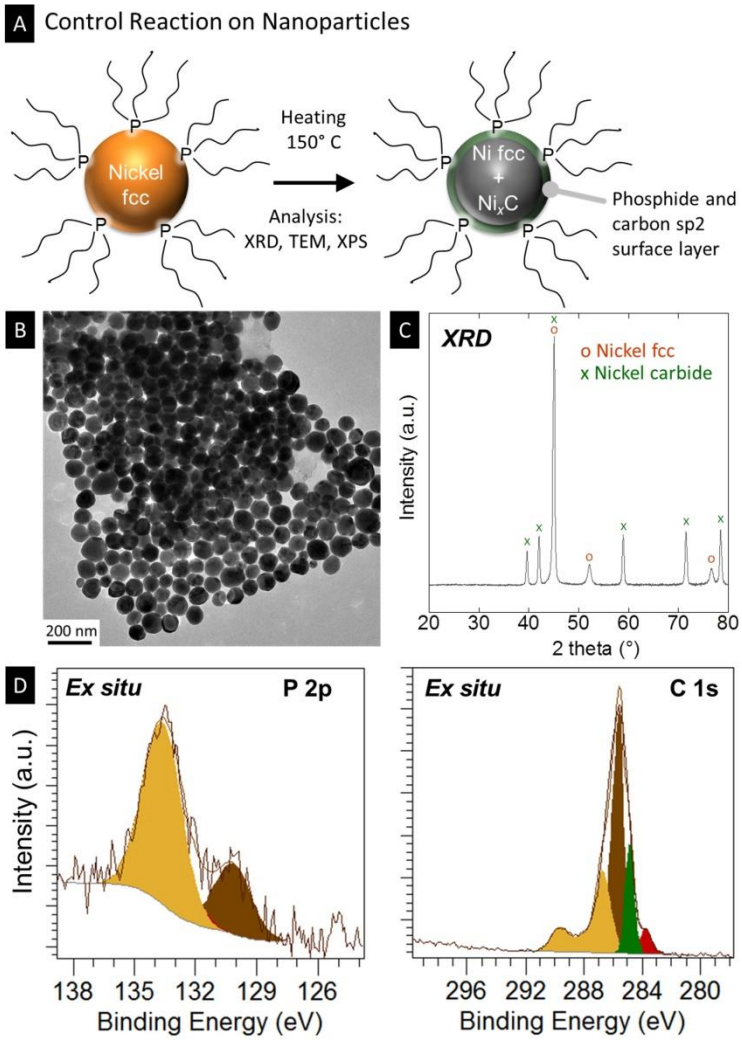

Figure 4: (A) Reaction scheme. (B) Transmission electron micrograph of resulting nanoparticles. (C) X-ray diffraction on the nanoparticles powder. (D) *Ex situ* XPS analysis of the resulting nanoparticles Color code is the following: P 2p: TOP on nickel in ochre, TOP on unsaturated sites in yellow, nickel phosphide in brown; C 1s: carbide in ochre, TOP alkyl chains in brown, all C-O species in yellow, sp2 carbon on nickel in green.

3. Conclusion

We have identified that 150 °C is the onset decomposition temperature of TOP on a nickel foil, which is a value significantly lower than that suggested in previous *ex situ* experiments. The formation of surface sp2 carbon was also uncovered. Considering the conductive character of sp2 carbon, this finding should be taken into account in discussing the properties of nickel phosphide nanoparticles in electro-catalysis. More generally, and because phosphines adsorb strongly also on several other transition

metals (Fe, Pd, Co, etc.), these findings suggests that metal(0) nanoparticles synthesis employing TOP could in many cases results in the formation of both phosphorus and carbon Ni compounds, not only above 200 °C,[32],[51] but also at temperatures as low as 150 °C, which we confirmed by performing a direct reaction of nickel(0) nanoparticles with TOP.

4. Experimental section

(i) Chemical state of the surface of the foil was analyzed *in situ* by ambient-pressure x-ray photoelectron spectroscopy (APXPS), which allows exposure of the sample to gas up to a few Torr. The experiments were conducted at beamline 9.3.2 of the Advanced Light Source in Berkeley, California.[38] All spectra were measured with a photon energy of 630 eV.[38] Fermi edge was use to calibrate the spectra. Details on the fitting procedure are available in the Supporting Information file.

(ii) *Foil preparation.* Prior to TOP adsorption, a high-purity foil of nickel from Goodfellows was cleaned by three sequences of sputtering and annealing. Sputtering was achieved under 1.10^{-5} Torr of Argon, with a tension of 1.5 kV and a current of 20 mA, for 30 minutes. Annealing was achieved at 400 °C under vacuum for 10 minutes.

(iii) *Deposition procedure for TOP.* In an inert glovebox (O_2 < 0.5 ppm and H_2O < 0.5 ppm), a diluted solution of TOP (Strem Chemicals, 98%) was prepared in dry and degassed toluene. Solution concentration was ca 5.10^{-2} mol/L. In the glovebag attached to the beamline chamber load-lock, 0.1 mL of this solution was deposited on the foil (1 cm^2), sitting on a kimwipe tissue, and left drying for one minute. The foil was then introduced back in the beamline in a chamber at a pressure below 10^{-7} mbar. It was transferred in the analysis chamber of the NAP-XPS apparatus.

(iv) Reaction of pre-formed nickel(0) nanoparticles with TOP. [$Ni(acac)_2$] (1.00 g, 3.9 mmol) was added to 39.0 mmol of oleylamine (10.4 g, 10 equivalents). The mixture was degassed and then heated at 220 °C for 1 hour under inert atmosphere, giving quickly a black solution. The mixture was cooled to room temperature and the nanoparticles were observed to aggregate on the magnetic bar, as expected from ref [52]. TOP (5 equiv. *vs.* nickel, 19.5 mmol, 8.7 mL) was added to the solution. The solution was heated at 150 °C for 4h. The product was not ferromagnetic. It was collected by centrifugation and

washed three times with acetone to give a black powder. Powder XRD patterns were recorded with a Brucker D8 X-ray diffractometer operating in the reflection mode at Cu Kα radiation. The nanoparticles were redispersed in hexanes for the preparation of the TEM grid. TEM was performed using a TECNAI Spirit G2. *Ex situ* XPS was performed on a Omicron Nanotechnology apparatus with a monochromated X-ray source at 1486.6 eV.

Acknowledgements:

This work was supported by the Director, Office of Science, Office of Basic Energy Sciences, Chemical Sciences, Geosciences, and Biosciences Division, under the Department of Energy Contract No. DE-AC02-05CH11231. Funding from the same contract for the ALS and beamline 9.3.2 is also acknowledged. UPMC, CNRS and Collège de France are also acknowledged for partial support of SC. SC thanks Christophe Calers for the measurements of *ex situ* XPS on colloids and Clément Larquet for the TEM analysis of the same sample.

Supporting Information Available: Fitting parameters for XPS, complementary XPS spectrum of the foil, complementary TEM on the nanoparticles.

Table of Content

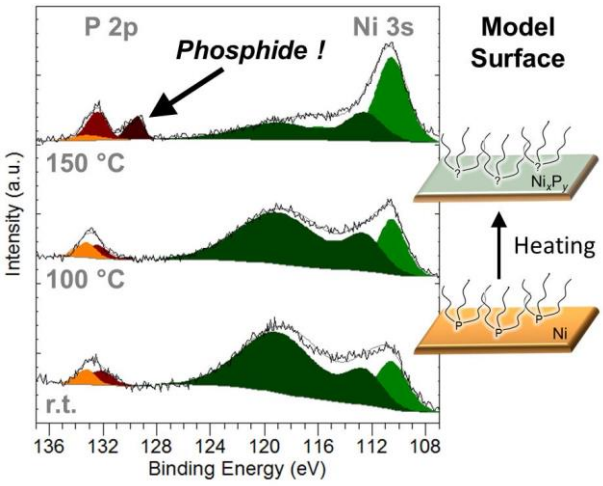

Mechanistic study of tri-n-octylphosphine (TOP) decomposition at a nickel surface shows phosphide formation at temperature as low as 150 °C, accompanied by sp2 carbon deposition. These two results were confirmed on nickel nanoparticles.

References

[1] V. Pralong, D. C. S. Souza, K. T. Leung, L. F. Nazar, *Electrochem. commun.* **2002**, *4*, 516–520.
[2] S. Carenco, C. Surcin, M. Morcrette, D. Larcher, N. Mézailles, C. Boissière, C. Sanchez, *Chem. Mater.* **2012**, *24*, 688–697.
[3] S. T. Oyama, T. Gott, H. Zhao, Y.-K. Lee, *Catal. Today* **2009**, *143*, 94–107.
[4] R. Prins, M. E. Bussell, *Catal. Letters* **2012**, *142*, 1413–1436.
[5] S. Carenco, A. Leyva-Pérez, P. Concepción, C. Boissière, N. Mézailles, C. Sanchez, A. Corma, *Nano Today* **2012**, *7*, 21–28.
[6] J. Baek, P. M. Allen, M. G. Bawendi, K. F. Jensen, *Angew. Chem. Int. Ed. Engl.* **2011**, *50*, 627–630.
[7] L. Li, P. Reiss, *J. Am. Chem. Soc.* **2008**, *130*, 11588–11589.
[8] R. a. Booth, M. Marinescu, J. Liu, S. a. Majetich, *J. Magn. Magn. Mater.* **2010**, *322*, 2571–2574.
[9] S. Carenco, X. F. Le Goff, J. Shi, L. Roiban, O. Ersen, C. Boissière, C. Sanchez, N. Mézailles, *Chem. Mater.* **2011**, *23*, 2270–2277.
[10] S. Carenco, D. Portehault, C. Boissière, N. Mézailles, C. Sanchez, *Chem. Rev.* **2013**, *113*, 7981–8065.
[11] E. J. Popczun, J. R. McKone, C. G. Read, A. J. Biacchi, A. M. Wiltrout, N. S. Lewis, R. E. Schaak, *J. Am. Chem. Soc.* **2013**, *135*, 9267–9270.
[12] Z. Pu, Q. Liu, C. Tang, A. M. Asiri, X. Sun, *Nanoscale* **2014**, *6*, 11031–11034.
[13] L. Feng, H. Vrubel, M. Bensimon, X. Hu, *Phys. Chem. Chem. Phys.* **2014**, *16*, 5917.
[14] E. J. Popczun, C. G. Read, C. W. Roske, N. S. Lewis, R. E. Schaak, *Angew. Chemie - Int. Ed.* **2014**, *53*, 5427–5430.
[15] L.-A. Stern, L. Feng, F. Song, X. Hu, *Energy Environ. Sci.* **2015**, *8*, 2347–2351.
[16] Z. Cai, X. Song, Y. Wang, X. Chen, *ChemElectroChem* **2015**, *2*, 1665–1671.
[17] Y. Shi, B. Zhang, *Chem. Soc. Rev.* **2016**, *45*, 1529–1541.
[18] B. You, N. Jiang, M. Sheng, M. W. Bhushan, Y. Sun, *ACS Catal.* **2016**, *6*, 714–721.
[19] N. Sweeny, C. Rohrer, O. Brown, *J. Am. Chem. Soc.* **1958**, *80*, 799–800.
[20] G. H. Layan Savithra, E. Muthuswamy, R. H. Bowker, B. A. Carrillo, M. E. Bussell, S. L. Brock, *Chem. Mater.* **2013**, *25*, 825–833.
[21] J.-G. J. Park, B. Koo, K. Y. Yoon, Y. Hwang, M. Kang, T. Hyeon, *J. Am. Chem. Soc.* **2005**, *127*, 8433–8440.
[22] R.-K. R.-T. Chiang, *Inorg. Chem.* **2007**, *46*, 369–371.
[23] H.-R. Seo, K.-S. Cho, Y.-K. Lee, *Mater. Sci. Eng. B* **2011**, *176*, 132–140.
[24] J. Wang, A. C. Johnston-Peck, J. B. Tracy, *Chem. Mater.* **2009**, *21*, 4462–4467.
[25] E. Muthuswamy, G. H. L. Savithra, S. L. Brock, *ACS Nano* **2011**, *5*, 2402–2411.
[26] E. Muthuswamy, S. L. Brock, *Chem. Commun. (Camb).* **2011**, *47*, 12334–12336.
[27] D.-H. Ha, L. M. Moreau, C. R. Bealing, H. Zhang, R. G. Hennig, R. D. Robinson, *J. Mater. Chem.* **2011**, *21*, 11498–11510.
[28] H.-R. Seo, K.-S. Cho, Y.-K. Lee, *Mater. Sci. Eng. B* **2011**, *176*, 132–140.
[29] S. Carenco, C. Boissière, L. Nicole, C. Sanchez, P. Le Floch, N. Mézailles, *Chem. Mater.* **2010**, *22*, 1340–1349.
[30] S. Carenco, S. Labouille, S. Bouchonnet, C. Boissière, X.-F. Le Goff, C. Sanchez, N. Mézailles, *Chem. Eur. J.* **2012**, *18*, 14165–73.
[31] L. M. Moreau, D. H. Ha, H. Zhang, R. Hovden, D. A. Muller, R. D. Robinson, *Chem. Mater.* **2013**, *25*, 2394–2403.
[32] L. M. Moreau, D.-H. Ha, C. R. Bealing, H. Zhang, R. G. Hennig, R. D. Robinson, *Nano Lett.* **2012**, *12*, 4530–9.
[33] K. Senevirathne, a. W. Burns, M. E. Bussell, S. L. Brock, *Adv. Funct. Mater.* **2007**, *17*, 3933–3939.
[34] C. N. R. Rao, H. S. S. Ramakrishna Matte, R. Voggu, A. Govindaraj, *Dalt. Trans.* **2012**, *41*,

5089.
[35] V. Iablokov, S. K. Beaumont, S. Alayoglu, V. V Pushkarev, C. Specht, J. Gao, A. P. Alivisatos, N. Kruse, G. A. Somorjai, *Nano Lett.* **2012**, *12*, 3091–6.
[36] S. Carenco, C.-H. Wu, A. Shavorskiy, S. Alayoglu, G. A. Somorjai, H. Bluhm, M. Salmeron, *Small* **2015**, *11*, 3045–3053.
[37] D. E. Starr, Z. Liu, M. Hävecker, A. Knop-Gericke, H. Bluhm, *Chem. Soc. Rev.* **2013**, *42*, 5833–5857.
[38] M. E. Grass, P. G. Karlsson, F. Aksoy, M. Lundqvist, B. Wannberg, B. S. Mun, Z. Hussain, Z. Liu, *Rev. Sci. Instrum.* **2010**, *81*, 53106.
[39] A. N. Mansour, *Surf. Sci. Spectra* **1994**, *3*, 211.
[40] M. Seno, S. Tsuchiya, T. Asahara, *Chem. Lett.* **1974**, *3*, 405–408.
[41] A. N. Mansour, *Surf. Sci. Spectra* **1994**, *3*, 231.
[42] E. Fluck, D. Weber, *Z. Naturforsch. B* **1974**, *29*, 603.
[43] Battistoni C., M. G., Z. R., N. L., *J. Electron Spectrosc. Relat. Phenom.* **1982**, *28*, 23.
[44] M. G. Thube, S. K. Kulkarni, D. Huerta, A. S. Nigavekar, *Phys. Rev. B* **1986**, *34*, 6874–6879.
[45] V. Nemoshkalenko, V. Didyk, V. Krivitskii, A. Senkevich, *Zhurnal Neorg. Khimii* **1983**, *28*, 2182–2186.
[46] P. E. Garrou, *Chem. Rev.* **1985**, *85*, 171–185.
[47] A. Acosta-Ramírez, M. Flores-Álamo, W. D. Jones, J. J. García, *Organometallics* **2008**, *27*, 1834–1840.
[48] C. Du, N. Pan, *Mater. Lett.* **2005**, *59*, 1678–1682.
[49] A. Moisala, A. G. Nasibulin, E. I. Kauppinen, *J. Phys. Condens. Matter* **2003**, *15*, S3011–S3035.
[50] M. Barber, J. A. Connor, L. M. R. Derrick, M. B. Hall, I. H. Hillier, *J. Chem. Soc., Faraday Trans. 2* **1973**, *69*, 559–562.
[51] Z. L. Schaefer, K. M. Weeber, R. Misra, P. Schiffer, R. E. Schaak, *Chem. Mater.* **2011**, *23*, 2475–2480.
[52] S. Carenco, C. Boissiere, L. Nicole, C. Sanchez, P. Le Floch, N. Mezailles, *Chem. Mater.* **2010**, *22*, 1340–1349.
[53] S. Carenco, S. Labouille, S. Bouchonnet, C. Boissière, X.-F. Le Goff, C. Sanchez, N. Mézailles, *Chem. Eur. J.* **2012**, *18*, 14165–73.